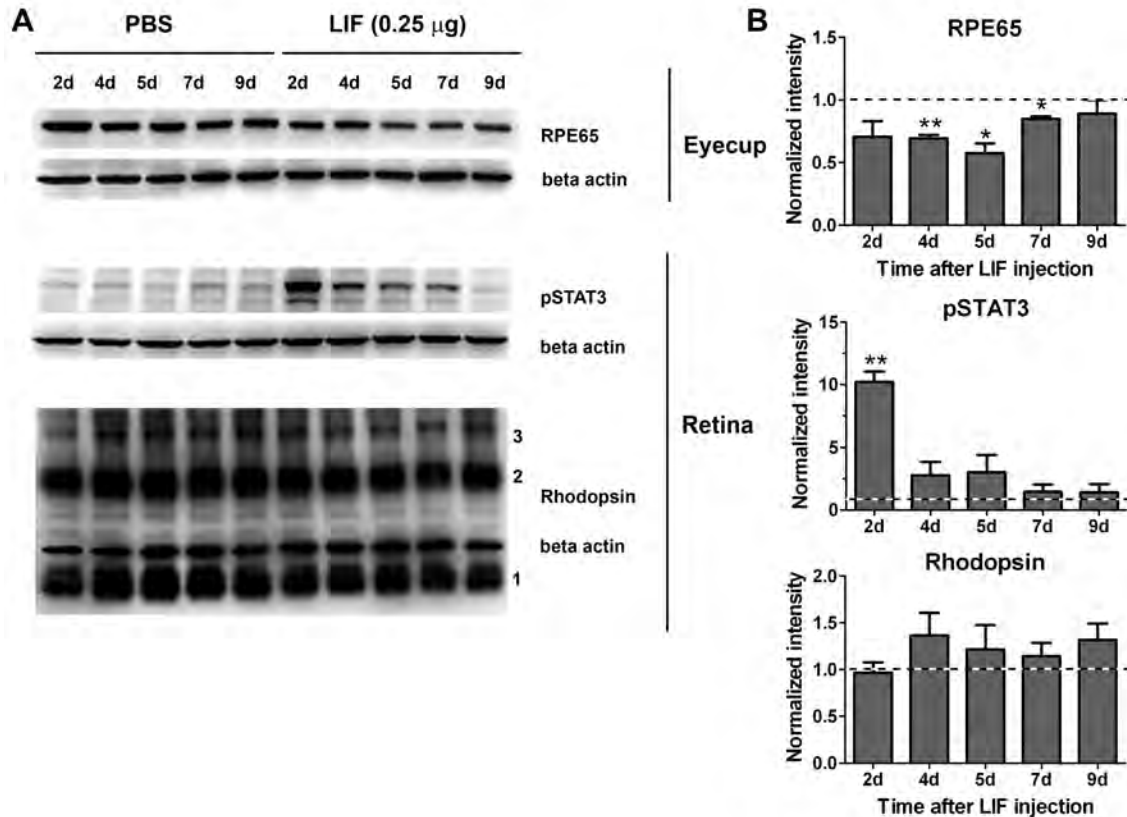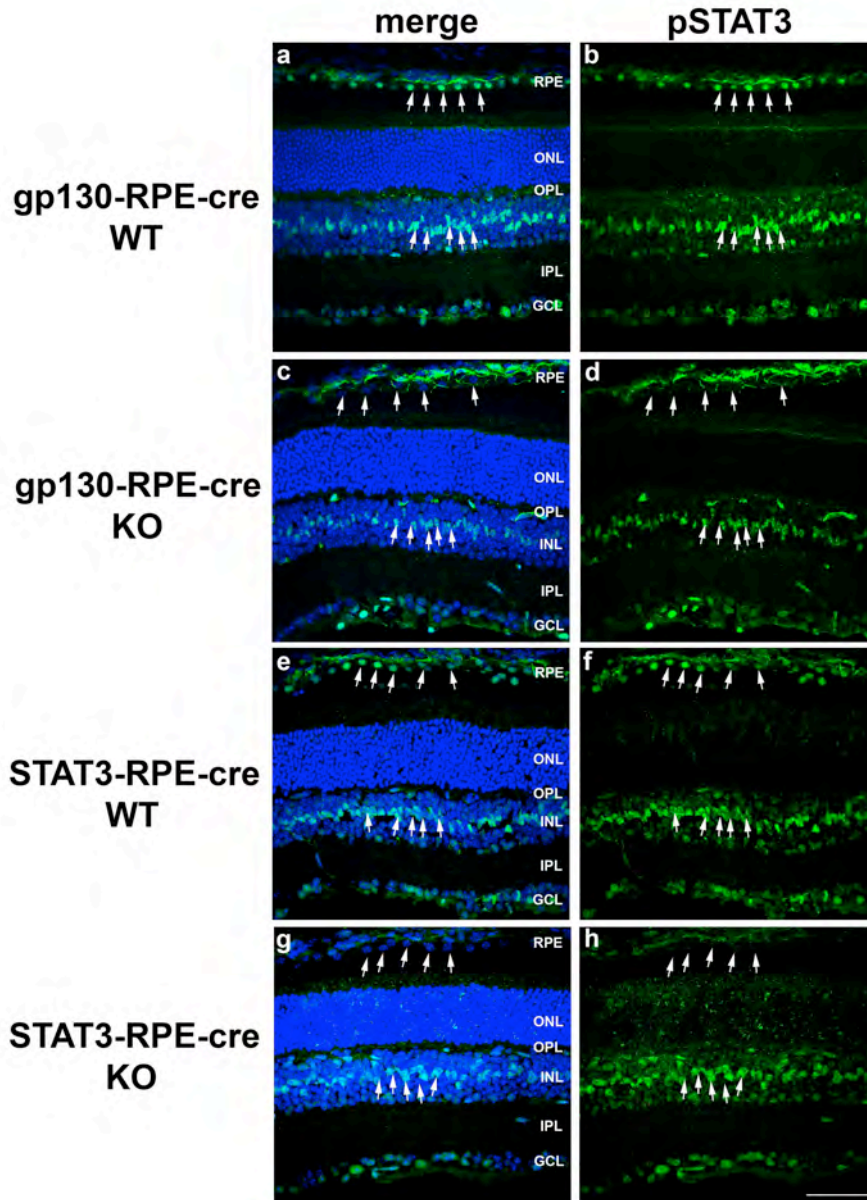**Supplemental Figure 1.**

Supplemental Figure 1. Low doses of LIF cause decreased levels of RPE65 protein.

Representative blots from eyecup and retina fractions showing decreased content of

RPE65 protein in the RPE fraction of Balb/cj mice at different time points after

intravitreal injection with 0.25μg (supplemental Fig 1*A*). In retina fractions from the same

mice, LIF treatment caused time-dependent activation of STAT3 and no significant

changes in rhodopsin protein content (supplemental Fig. 1*B*). β-actin was used as loading

control. Normalizations were done to the respective PBS control. (n= 3 for each group;

comparing LIF-injected eyes to their respective PBS controls, * p < 0.05 by paired *t*-test.

Error bars, SEM).
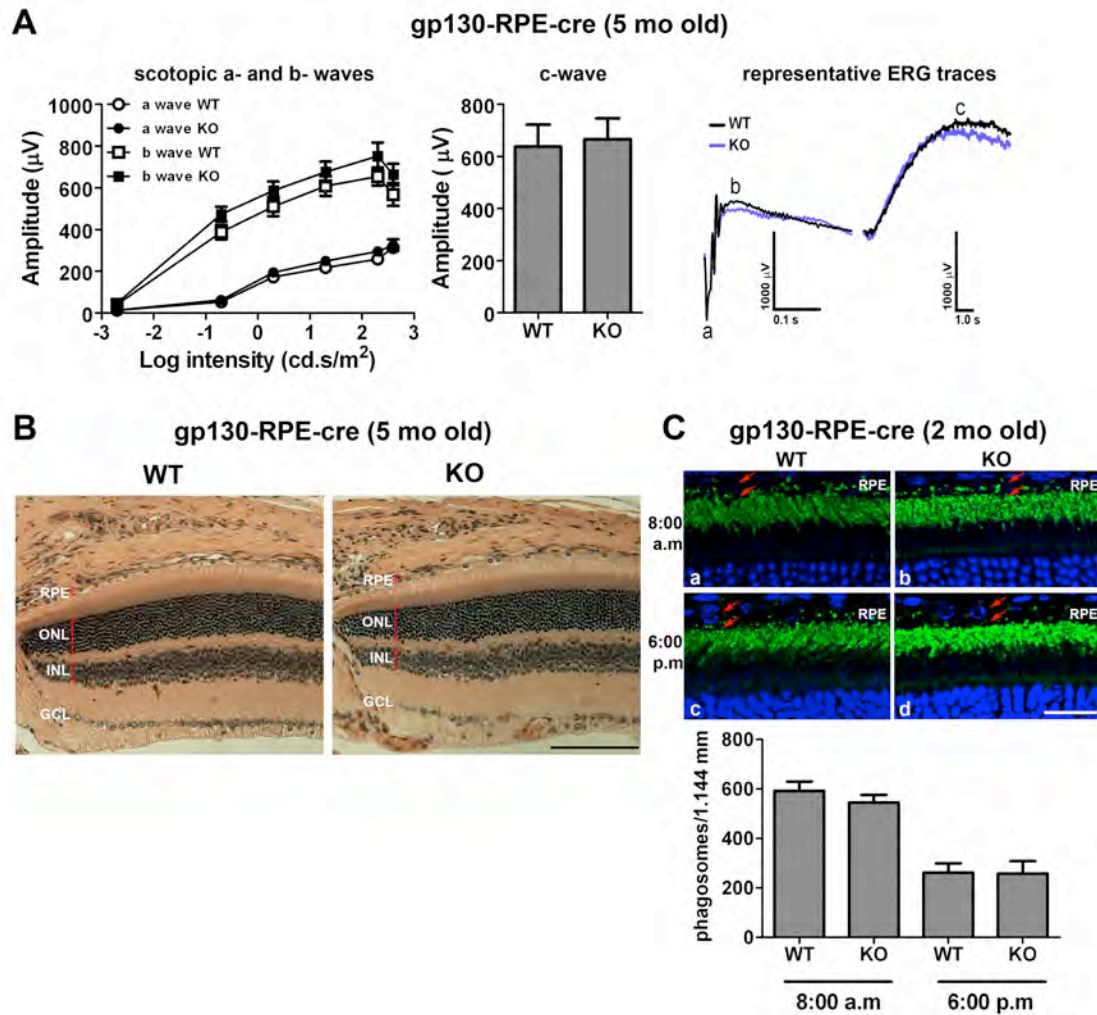
Supplemental Figure 2

Supplemental figure 2. Specificity of deletion of gp130 in the conditional gp130-RPE-cre KO and of STAT3 in the in the STAT3-RPE-cre KO mouse models.

The specificity of deletion for gp130 and STAT3 in both RPE-specific conditional KO mice was demonstrated by IHC on frozen retinal sections using anti-pSTAT3 antibody

(green). Following 30 min after single intravitreal injection of 0.5μg LIF, robust activation of STAT3 was observed in both RPE cells and neuroretina (mostly Müller cells) of gp130-RPE-cre WT (a) and STAT3-RPE-cre WT (f) eyes. In comparison, in the eyes of gp130-RPE-cre KO (d) and STAT3-RPE-cre KO (h) mice, pSTAT3 signal was absent in RPE cells and still maintained in the neuroretina. Merged images of pSTAT3 and DAPI are shown (a, c, e, g).; RPE, retinal pigmented epithelium; ONL, outer nuclear layer; OPL, outer plexiform layer; INL, inner nuclear layer; IPL, inner plexiform layer; GCL, ganglion cell layer. Scale bar, 200 μm.
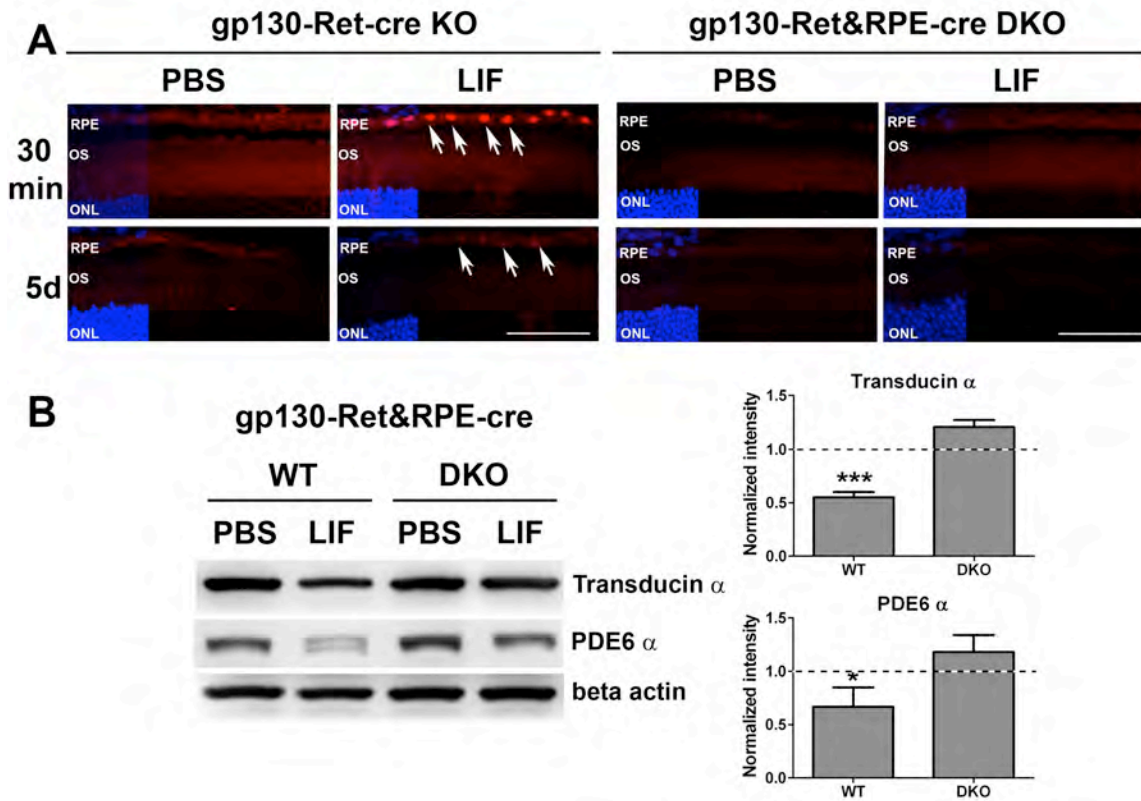
Supplemental Figure 3.

Supplemental Figure 3. Gp130-RPE-cre KO mice exhibit normal ERG responses, morphology, and RPE phagocytic function. A) Scotopic a- and b- ERG responses to increasing flash intensities (lines graph), and c-wave driven response after a single flash of intensity (bars graph) in gp130-RPE-cre-KO were indistinguishable from their WT littermate control mice. Representative ERG traces are shown for both WT and KO. (n= at least 5 for each group. Error bars, SEM). B) Representative images at the superior retina near the optic nerve head show normal retinal morphology in the 5 month-old

gp130-cre-KO mouse, compared to WT littermate. Scale bar, 100 μm. C)

Immunohistochemical detection of opsin-labeled phagosomes in RPE cells (rhodopsin;

green) on paraffin retinal sections of 2 month-old gp130-RPE-cre KO mice.Eyes were

collected at the time points indicated (8:00 a.m (a, b) and 6:00 p.m (c, d)). The red

arrows depict the apical and basal margins of the RPE. Nuclei were counterstained with

DAPI (blue). Scale bar, 20 μm. The bar graph in C shows the quantification of

phagocytic activity of RPE, at 8:00 a.m and 6:00 p.m expressed as number of

phagosomes in RPE. Compared to WT littermates, gp130-RPE-cre KO did not change

significantly the number of phagosomes in RPE cells at any of the collection times

studied (n= 4 for each group. Error bars, SEM).
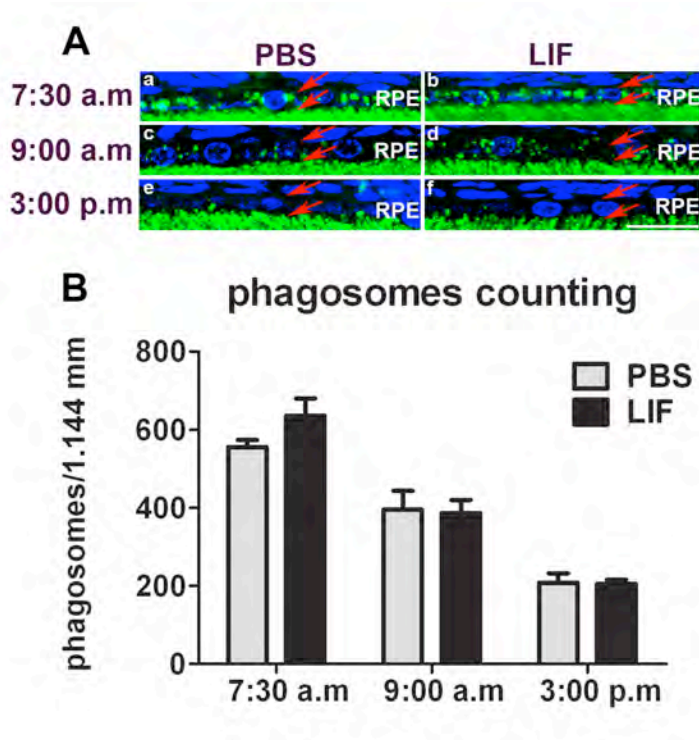
Supplemental Figure 4.

Supplemental Figure 4. In the absence of gp130 in both retina and RPE, LIF does not activate STAT3 nor affect the expression levels of phototransduction proteins. A) Immunohistochemical detection of STAT3 activation (pSTAT3; red) on frozen retinal sections of gp130- Ret-cre KO and gp130-Ret&RPE-cre DKO after 30 min, and 5 days of intravitreal injection with LIF and PBS. While in the gp130-deleted retina STAT3 is robustly activated in RPE cells, the double deletion of gp130 in retina and RPE shows no activation of STAT3 by LIF. Scale bar, 200 μm. B) Representative blots and densitometry analysis of transducin- α and PDE6-α proteins content from retina homogenates, 5 days after intravitreal injection of 3.0 μg LIF. The decreased content of

these proteins by LIF in the WT controls was abolished by the double deletion of gp130 in retina and RPE. Beta- actin was used as loading control. Normalizations were done to the respective PBS control and used for comparisons between WT and DKO groups (n= 3 for each group, * and *** $p < 0.05$ by unpaired *t*-test. Error bars, SEM).
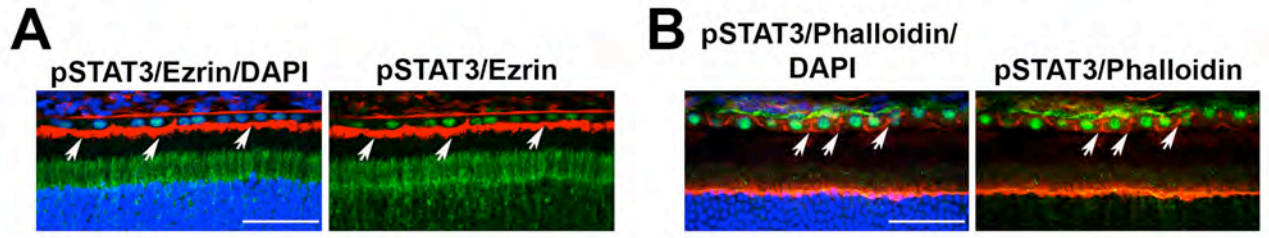
Supplemental Figure 5.

Supplemental Figure 5. LIF does not alter the phagocytosis of rod outer segments in RPE. A) Immunohistochemical detection of opsin-labeled phagosomes in RPE cells (rhodopsin; green) on paraffin retinal sections of gp130-Ret KO mice. Eyes were collected 5 days after a single intravitreal injection of 3μg LIF (b, d, f) or PBS (a, c, e). Eyes were collected at the time points indicated (7:30 a.m (a, b); 9:00 a.m (c, d); and 3:00 p.m (e, f)). The red arrows depict the apical and basal margins of the RPE. Nuclei were counterstained with DAPI (blue). Scale bar, 20 μm. B) Quantification of phagocytic activity of RPE, 5 days after 3.0 μg LIF and PBS intravitreal injections of gp130-Ret-cre KO mice at different time points of the day, expressed as number of phagosomes in RPE. Compared to PBS, LIF did not change significantly the number of phagosomes in RPE cells at any of the collection times (n= 4, comparing PBS and LIF-injected eyes. Error bars, SEM).
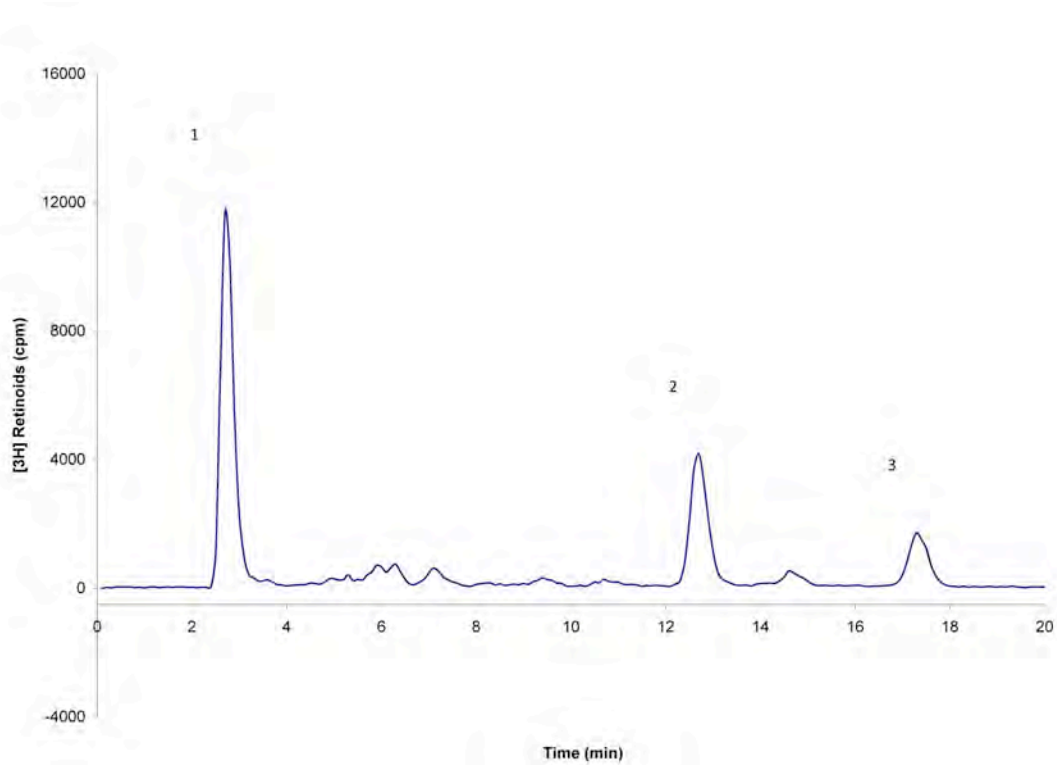
Supplemental Figure 6.

Supplemental Figure 6. Markers used to localize activation of STAT3 to RPE nuclei following intravitreal injections of LIF.

Co-staining of retinal frozen sections with anti-pSTAT3 (green label) and anti-Ezrin (red label in A) or Phalloidin (red label in B), which labels the circumferential actin cytoskeleton in RPE served to localize activated STAT3 to RPE nuclei upon intravitreal injections of LIF. Scale: 50 μm.

Supplemental Figure 7.

Supplemental Figure 7. Representative HPLC retinoid profile for a not injected

Balb/cj mouse

Representative peaks were identified as follows: 1 , retinyl esters, 2, 11-*cis* retinol, 3, all-

trans retinol**.**

Supplemental table 1.

Primers sequence (5'→ 3')

RPE65 for: CAC TGT GGT CTC TGC TAT CTT C
RPE65 rev: GGT GCA GTT CCA CTT CAG TT

Rd1 for: CAT CCC ACC TGA GCT CAC AGA AAG
Rd1 rev: GCC TAC AAC AGA GGA GCT TCT AGC

STAT3 a: CCT GAA GAC CAA GTT CAT CTG TGT GAC
STAT3 b: CAC ACA AGC CAT CAA ACT CTG GTC TCC

Gp130 for: ACG TCA CAG AGC TGA GTG ATG CAC
Gp130 rev: GGC TTT TCC TCT GGT TCT TG

VMD2cre for: CGG CCT TGA ATT GAT CAT ATG CGG
VMD2cre rev: TCA AAC TCG AAG TCG GCC ATA TCC

Chx10cre for: GGG CAC CTG GGA CCA ACT TCA CGA
Chx10cre rev: CGG CGG CGG TCA CGA ACT CC

Cre for: AGG TGT AGA GAA GGC ACT TAG C
Cre rev: CTA ATC GCC ATC TTC CAG CAG G

Supplemental table 1. Sequences of primer sets used for PCR genotyping.

Supplemental table 2.

Primers sequence (5'→ 3')

RPE65 for: TGG ATC TCT GTT GCT GGA AAG GGT
RPE65 rev: TCT GCC TGT GTC GAC CTT GTC A AT

LRAT for: AGC CTA CTG TGG AAC AAC TGC GAA
LRAT rev: TGA TGC CAG GCC TGT GTA GAC AAT

RDH5 for: TCT GGC ACT GCA ACT TGA CCA GAA
RDH5 rev: TTC TCC AAC ACG TGT CTT CAC CCA

RGR for: GGT TTC CAG GGA TTT GCA ACA GCA
RGR rev: ACA TCC ACA CAA ACA GCA CCA GAG

IRBP for: AGA GCC GAT ATG CAA GGG TGA CTT
IRBP rev: TCG GTC TTT GGC ATC CTC TGG AAT

RPL19 for: TCA CAG CCT GTA CCT GAA GG
RPL19 rev: TCG TGC TTC CTT GGT CTT AG

Supplemental table 2. Sequences of primer sets used for qRT-PCR.